Double-folding nucleus-nucleus potential based on the self-consistent calculations

1. Introduction
2. Nucleus-nucleus interaction potentials
3. EDF for nuclear ground-state density profiles
4. Useful parameterization
5. Coulomb barriers and sub-barrier fusion
6. Modification of Skyrme EDF
7. Summary

G.Adamian, N.Antonenko, V.Sargsyan, H.Lenske
A.Severyukhin, N.Arsenyev

-EDF and nuclear properties. The central density and radius are mainly related to the internal NN forces.

-The diffuseness of the nuclear surface is related to the external part of NN forces or to the effect of finite Fermi-system.

-Nucleus-nucleus potentials (hight and position of the Coulomb barrier).

-Sub-barrier fusion in astrophysical reactions.

Self-consistent approaches: relativistic and non-relativistic Micro-macro models

RMF [J. Meng, H. Toki, S.G. Zhou, S.Q. Zhang, W.H. Long, and L.S. Geng, Prog. Part. Nucl. Phys. **57**, 470 (2006)]

The non-covariant EDFs. The fit of these EDFs involves binding energies, Q_α-values in heavy and superheavy nuclei, and nuclear structure effects. The equilibrium deformations are determined by the minimization of the total energy of the system.
SV-bas [P. Klupfel, P.-G. Reinhard, T.J. Buervenich, and J.A. Maruhn, PRC **79**, 034310 (2009)]
Giessen EDF [F.Hofmann and H.Lenske, PRC 57, 2281 (1998)]

MM models [P.Möller *et al.*; A.Sobiczewski *et al.*; P.Jachimowicz, M.Kowal, and J.Skalski, At. Data Nucl. Data Tables **138**, 101393 (2021); Lublin model] provide stronger shell effects at Z = 114 and N = 184.
With the TCSM (like in the RMF and Skyrme self-consistent treatments) the proton shell closure is expected at Z = 120-126 and there are strong shell effects at N = 184.

The nucleus-nucleus interaction potential V is represented as the sum

$$V(R) = V_C(R) + V_N(R) + V_R(R)$$

of the Coulomb, nuclear, and centrifugal potentials.

The double-folding procedure

$$V_N(R) = \int d\mathbf{r_1} d\mathbf{r_2}\, \rho_1(\mathbf{r_1})\rho_2(\mathbf{R}-\mathbf{r_2})F(\mathbf{r_2}-\mathbf{r_1}).$$

The effective *NN* forces

$$F(\mathbf{r_2}-\mathbf{r_1}) = C_0\left(F_{in}x(\mathbf{r_1}) + F_{ex}\left(1-x(\mathbf{r_1})\right)\right)\delta(\mathbf{r_2}-\mathbf{r_1}),$$

$$x(\mathbf{r_1}) = \rho_1(\mathbf{r_1}) + \rho_2(\mathbf{R}-\mathbf{r_2})$$

The Landau-Migdal parameters F_{in} and F_{ex}, C_0 are determined from a fit to experimentally measured properties of nuclei

$$F = \frac{\delta^2 \mathcal{E}_{int}(x)}{\delta x^2} = C_0[F_{ex} + (F_{in} - F_{ex})x] \qquad \text{the Giessen EDF}$$

$$C_0 = 308\ \text{MeV/fm}^3 \quad \rho_0 = 0.16\ \text{fm}^{-3} \quad F_{ex} = -3.84 \quad F_{in} = 0.09$$

With a radial-dependent effective mass m_q^* the equation for the single-particle wave function is as follows

$$\left(-\boldsymbol{\nabla}\cdot\frac{\hbar^2}{2m_q^*(\mathbf{r})}\boldsymbol{\nabla}+V_q(\mathbf{r})+V_q^{(ls)}(\mathbf{r})-\varepsilon_q\right)\psi_q(\mathbf{r})=0.$$

The self-consistent approaches lead to single-particle potentials given in non-relativistic formulation by

$$U_q(\rho)=V_q(\rho)+V_q^{(ls)}(\rho)=\frac{\hbar^2k_{\mathrm{F}_q}^2}{2m_q}\left(1-\frac{m_q}{m_q^*}\right)+\Sigma_q(k_{\mathrm{F}_q},\rho)+V_q^{(ls)}(\rho)$$

$\Sigma_q(k,\rho)$ - self-energies, k_{F_q} - wave number at the Fermi surface, m_q – bare nucleon mass. Reduction to the standard Schrödinger equation [EPJA 54, 170 (2018); 57, 89 (2021)]

$$\left(-\frac{\hbar^2}{2m_q}\boldsymbol{\nabla}^2+U_q(r)+U_q^{(ls)}(r)-\varepsilon_q\right)\psi_q(r)=0,$$

$$U_q(r)=V_q(r)+\frac{\hbar^2}{2m_q}\mu_q(r)\bar{k}_{\mathrm{eff}}+\frac{3}{5}\left(1-\frac{m_q^*(r)}{m_q}\right)\frac{\hbar^2k_{\mathrm{F}_q}^2(r)}{2m_q^*(r)}$$

$$U_q^{(ls)}(r)=\frac{m_q^*(r)}{m_q}V_q^{(ls)}(r)=-\frac{1}{m_q}\frac{1}{r}\frac{\mathrm{d}\ln(m_q^*(r)/m_q)}{\mathrm{d}r}\mathbf{l}\cdot\mathbf{s}$$

Giessen EDF for nuclear ground-state density profiles

Nuclear binding energies, single-particle states, and ground-state densities are described by an energy density functional

$$\mathcal{E}(\rho_q, \tau_q, \kappa_q) = \mathcal{E}_{kin}(\tau_q) + \frac{1}{2}\mathcal{E}_{int}(\rho_q) + \frac{1}{2}\mathcal{E}_{pair}(\rho_q, \kappa_q) - \sum_{q=p,n} \lambda_q \rho_q$$

The proton (q = p) and neutron (q = n) densities

$$\rho_q = \sum_{jm} v_{jm}^2 |\varphi_{qjm}|^2,$$

corresponding kinetic energy densities

$$\tau_q = \sum_{jm} v_{jm}^2 \frac{\hbar^2}{2m_q} |\nabla \varphi_{qjm}|^2,$$

and pairing densities,

$$\kappa_q = \frac{1}{2} \sum_{jm} u_{jm} v_{jm} |\varphi_{qjm}|^2.$$

Nucleon density distribution

The nucleon density distribution in the spherical nucleus is usually taken in the three-parameter symmetrized Fermi-type form

$$\rho(r) = \frac{\rho_0}{1 + \exp[(r - R)/a]},$$

where ρ_0 is the saturated nucleon density in the center of nucleus, $R = r_0 A^{1/3}$ is the nuclear radius with the parameter r_0, and a is the nuclear diffuseness.

The value of

$$\rho_0 = \frac{3}{4\pi r_0^3} \frac{1}{1 + \left(\frac{\pi a}{r_0 A^{1/3}}\right)^2},$$

provides the proper normalization. Two-parameter fit of the nuclear density profile provides r_0= 1.073 and 1.081 fm, a=0.538 and 0.53 fm for ^{40}Ca and ^{48}Ca, respectively.

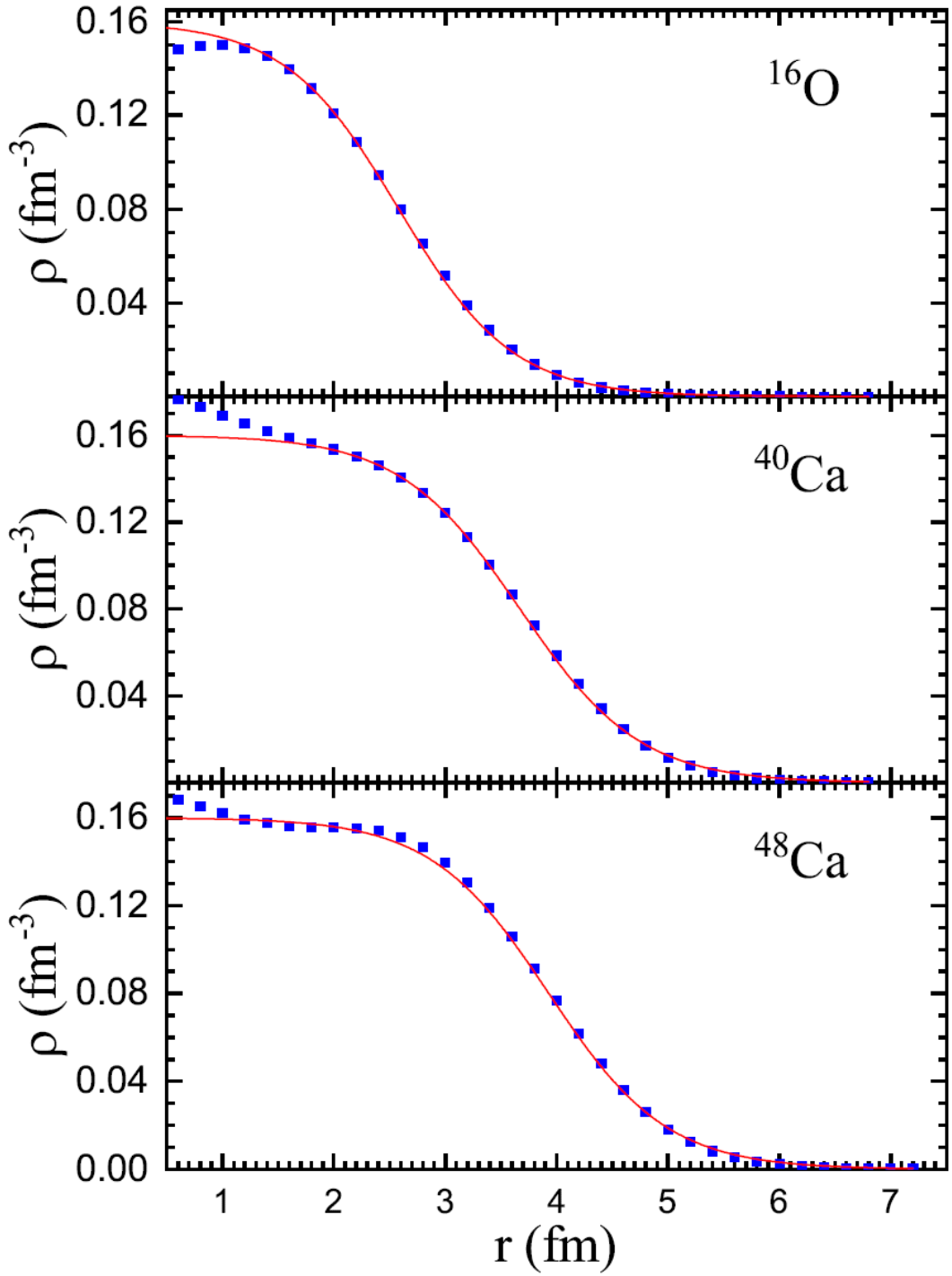

Self-consistent HFB nucleon-density distributions (symbols) in indicated spherical nuclei are fitted by the Fermi-type form where always $\rho_0 = 0.16$ fm^{-3} (lines).

Useful parameterizations

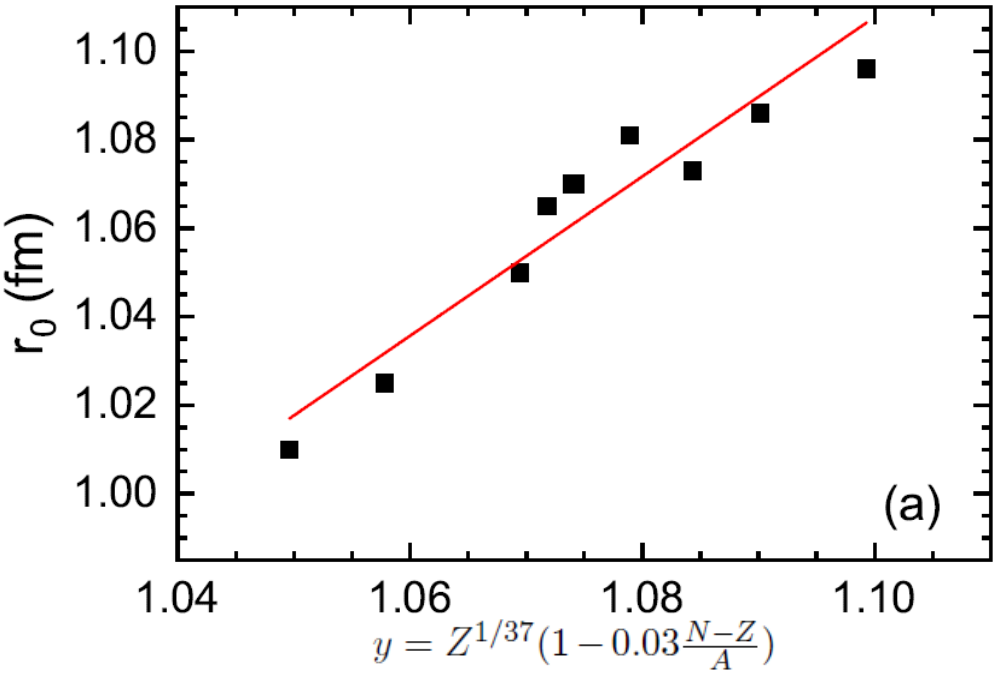

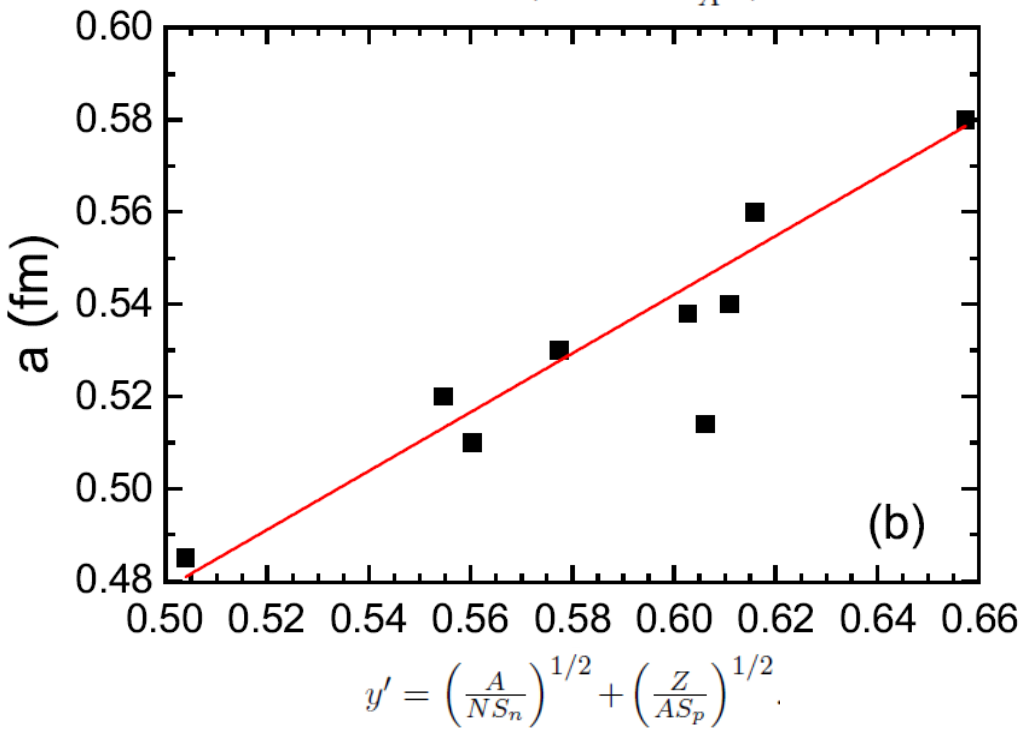

$$r_0 = 1.8Z^{1/37}\left(1 - 0.03\frac{N-Z}{A}\right) - 0.87 \text{ [fm]},$$

$$a = 0.64\left[\left(\frac{A}{NS_n}\right)^{1/2} + \left(\frac{Z}{AS_p}\right)^{1/2}\right] + 0.16 \text{ [fm]}$$

PARAMETERIZATION OF THE NUCLEAR PART OF NUCLEUS-NUCLEUS INTERACTION POTENTIAL

For spherical nuclei, the nuclear part of nucleus-nucleus interaction potential can be parameterized by the Morse-type potential

$$V_N(R) = D\left[\exp\left(-2\frac{R-R'_0}{d}\right) - 2\exp\left(-\frac{R-R'_0}{d}\right)\right].$$

A good description of the heights of the Coulomb barriers is achieved at

$$\begin{aligned} D &= 49.3\frac{R_{01}R_{02}}{R_{01}+R_{02}}\sqrt{\frac{a_1a_2}{a_1+a_2}}, && \text{[MeV]} \\ R'_0 &= 0.98(R_{01}+R_{02})\sqrt{a_1+a_2}, && \text{[fm]} \\ d &= 0.8\sqrt{a_1+a_2}, && \text{[fm]} \end{aligned}$$

Coulomb barriers and sub-barrier fusion

TABLE I: The calculated values of V_b, R_b, and $\omega_b = \sqrt{\frac{1}{\mu}\frac{d^2V(R)}{dR^2}|_{R=R_b}}$ are compared with those for phenomenologically adjusted potentials in Ref. [23]. The nuclei are assumed to be spherical.

Reaction	R_b (fm)		V_b (MeV)		ω_b (MeV)	
	[23]	calc	[23]	calc	[23]	calc
$^{12}C + ^{12}C$	7.95	8.06	6.00	5.94	2.67	2.70
$^{12}C + ^{16}O$	8.32	8.32	7.64	7.67	2.68	2.77
$^{12}C + ^{30}Si$	8.71	8.79	12.81	12.75	3.00	3.07
$^{16}O + ^{16}O$	8.69	8.57	9.75	9.94	2.67	2.82
$^{28}Si + ^{28}Si$	9.08	9.05	28.64	28.95	3.27	3.50
$^{28}Si + ^{30}Si$	9.28	9.27	28.07	28.27	3.16	3.33
$^{30}Si + ^{30}Si$	9.45	9.49	27.52	27.32	3.04	3.16
$^{24}Mg + ^{30}Si$	9.28	9.31	24.07	24.09	3.06	3.16
$^{40}Ca + ^{40}Ca$	10.08	9.99	52.46	53.34	3.22	3.47
$^{48}Ca + ^{48}Ca$	10.58	10.59	50.46	50.69	2.95	3.08
$^{36}S + ^{48}Ca$	10.34	10.29	41.20	41.65	2.90	3.09
$^{36}S + ^{64}Ni$	10.70	10.62	55.68	56.45	3.03	3.24

[23] Physics Letters B 824 (2022) 136792

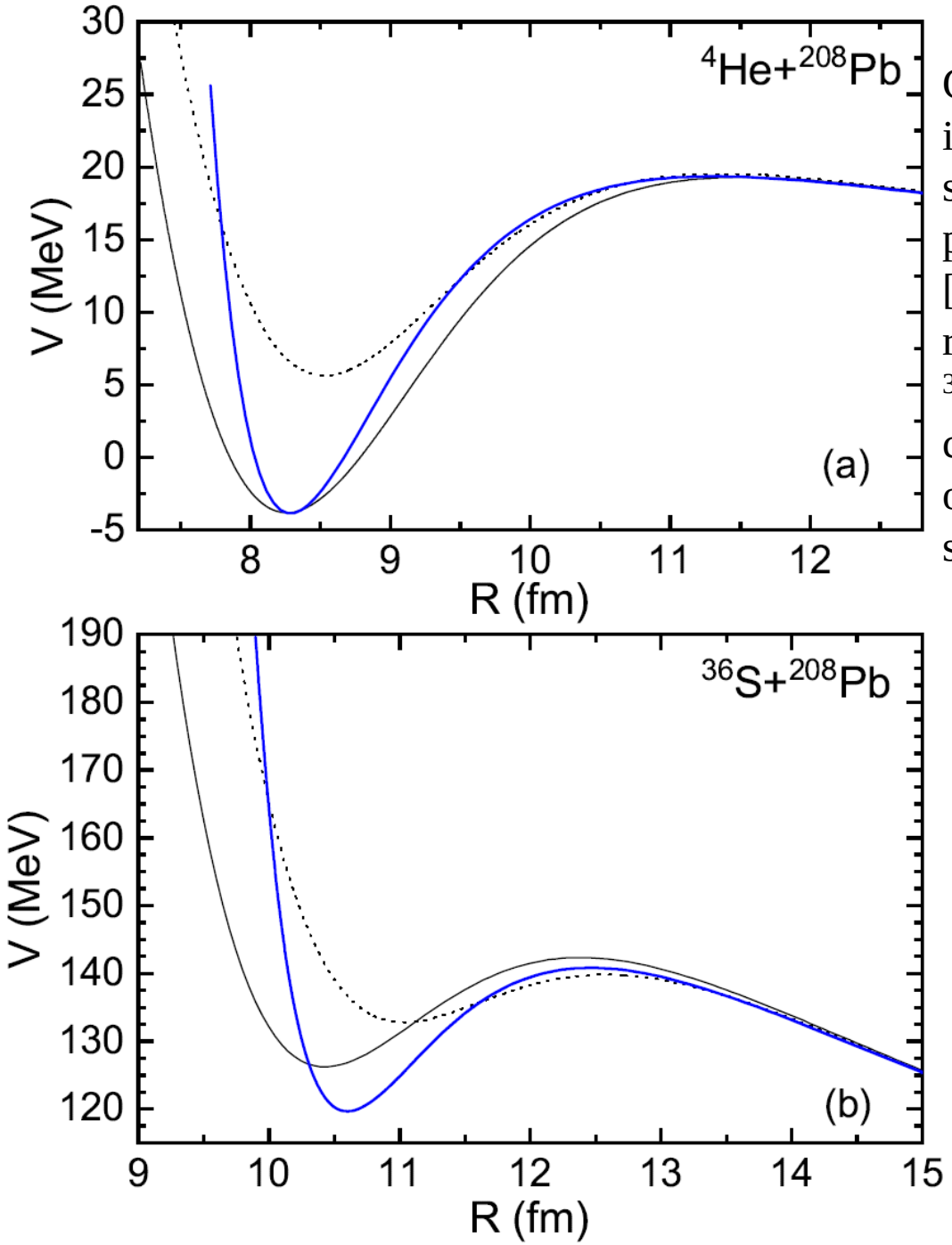

Comparison of nucleus-nucleus interaction potentials calculated with self-consistent (solid lines) and phenomenological (dashed lines) [23] nucleon densities for the reactions ^{4}He+^{208}Pb (a) and ^{36}S+^{208}Pb (b). The results of calculation with the parametrization of the nuclear part of the potential are shown by blue lines.

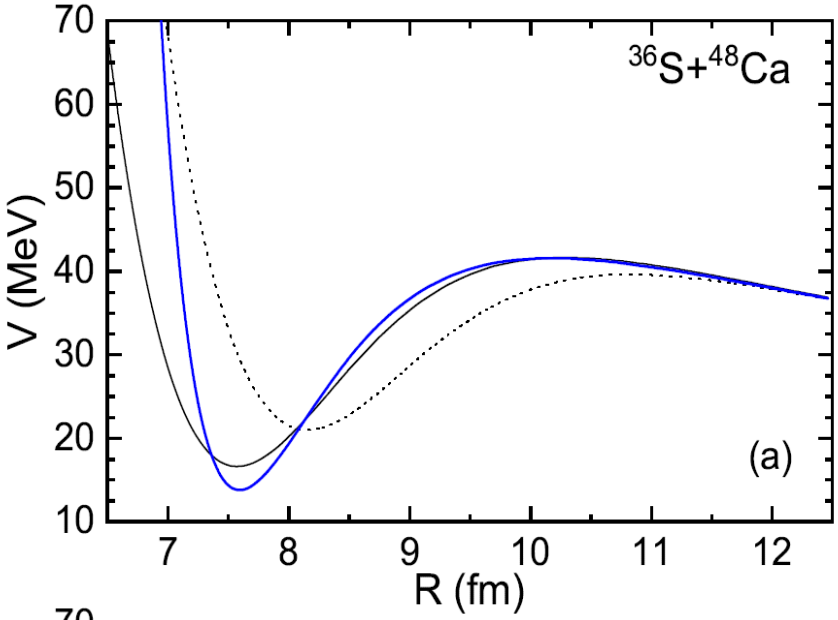
$^{36}S+^{48}Ca$
(a)
V (MeV)
R (fm)

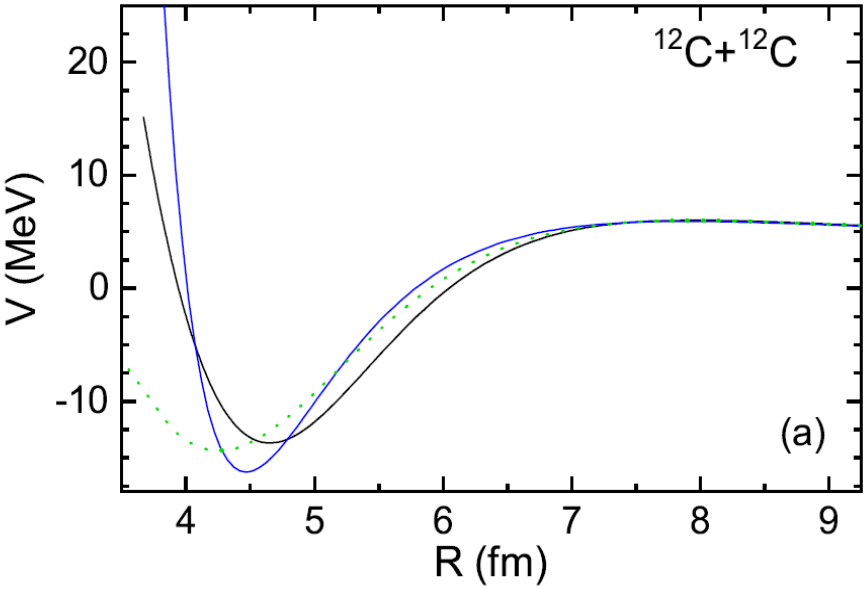
$^{12}C+^{12}C$
(a)
V (MeV)
R (fm)

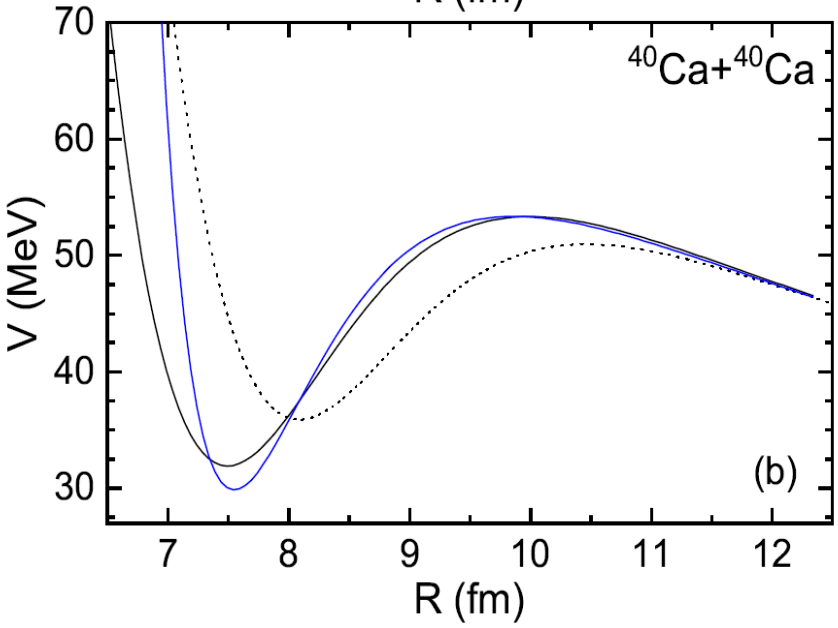
$^{40}Ca+^{40}Ca$
(b)
V (MeV)
R (fm)

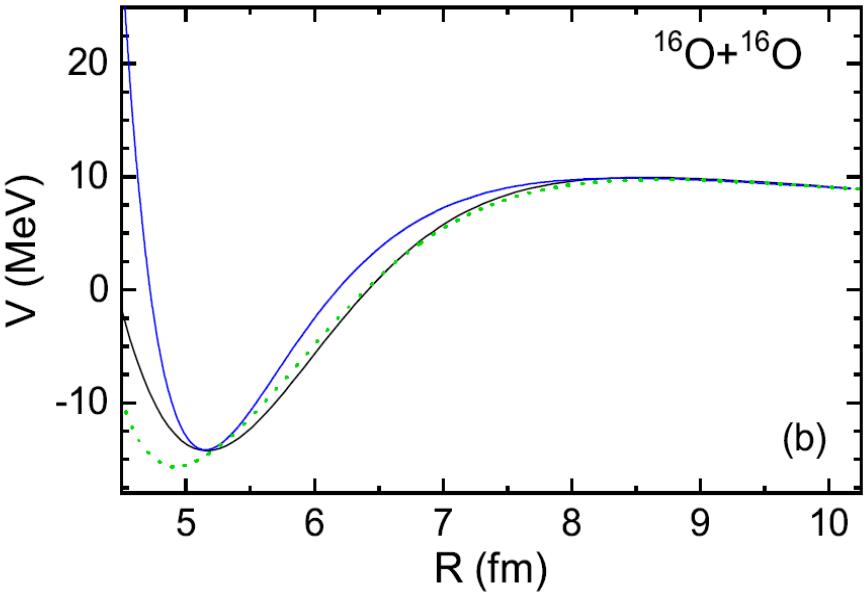
$^{16}O+^{16}O$
(b)
V (MeV)
R (fm)

For low-energy reactions with light- and medium-mass nuclei, the fusion cross section at the given center-of-mass energy $E_{\mathrm{c.m.}}$ is written as a sum over partial waves l

$$\sigma(E_{\mathrm{c.m.}}) = \frac{\pi\hbar^2}{2\mu E_{\mathrm{c.m.}}} \sum_l (2l+1)\bar{P}_l(E_{\mathrm{c.m.}}),$$

$$\bar{P}_l = \int_0^{\pi/2}\int_0^{\pi/2} d\cos\theta_1 d\cos\theta_2\, P_l(E_{\mathrm{c.m.}}, \theta_1, \theta_2),$$

$$P_l = \frac{1}{2}\mathrm{erfc}\left[\sqrt{\frac{\pi(V_b - E_{\mathrm{c.m.}})}{\kappa\hbar\omega}}\right], \qquad \kappa = \sqrt{\frac{2V_b}{\mu\omega_b^2(R_1+R_2)^2 - 2V_b}}$$

$$\omega = \left(\frac{2[V_b - E_{\mathrm{c.m.}}]}{\mu[R_{\mathrm{ext}} - R_b]^2}\right)^{1/2},$$

R_{ext}, R_b and V_b are the external turning point, the position and height of the Coulomb barrier, respectively.

Physics Letters B 824 (2022) 136792

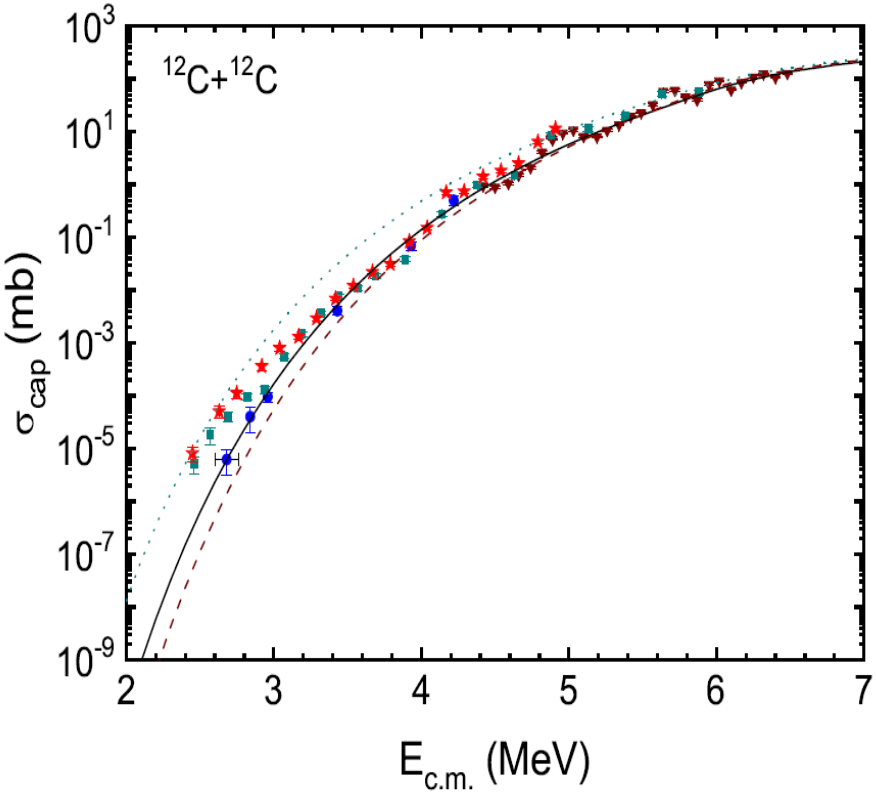

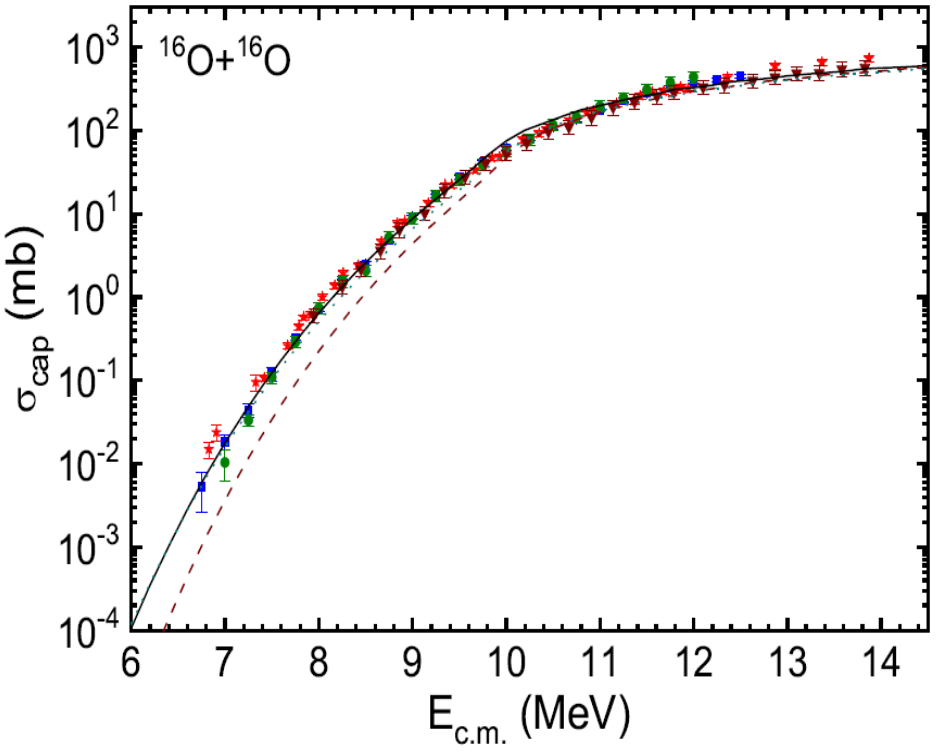

The fusion excitation functions calculated with phenomenologically adjusted (*solid lines*), self-consistent (*dashed line*), and parameterized (*dotted line*) potentials for the $^{12}C+ ^{12}C$ reaction. The experimental data are taken from [PRC 97, 012801(R) (2018)] (blue symbols), [PRC 73, 064601 (2006)] (black symbols), [PRL 124, 192701 (2020)] (red symbols), [PRL 124, 192702 (2020)] (wine symbols), [PRL 98, 122501 (2007)] (green symbols).

The experimental data are taken from [PRC 31, 1980 (1985)] (black symbols), [Z. Phys. A297, 161 (1980)] (blue symbols), [NPA 422, 373 (1984)] (red symbols) and [PRC 35, 591 (1987)] (wine symbols).

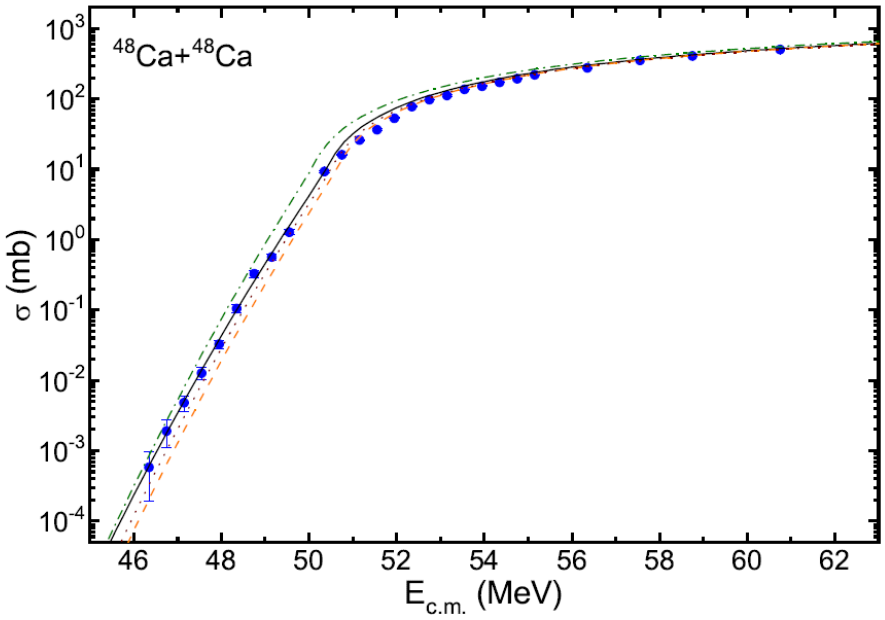

The experimental data are taken from [PLB 679, 95 (2009)] (symbols). The cross sections calculated with the self-consistent nucleus-nucleus potential obtained with F_{ex} = - 4.484 are shown by dash-dotted line.

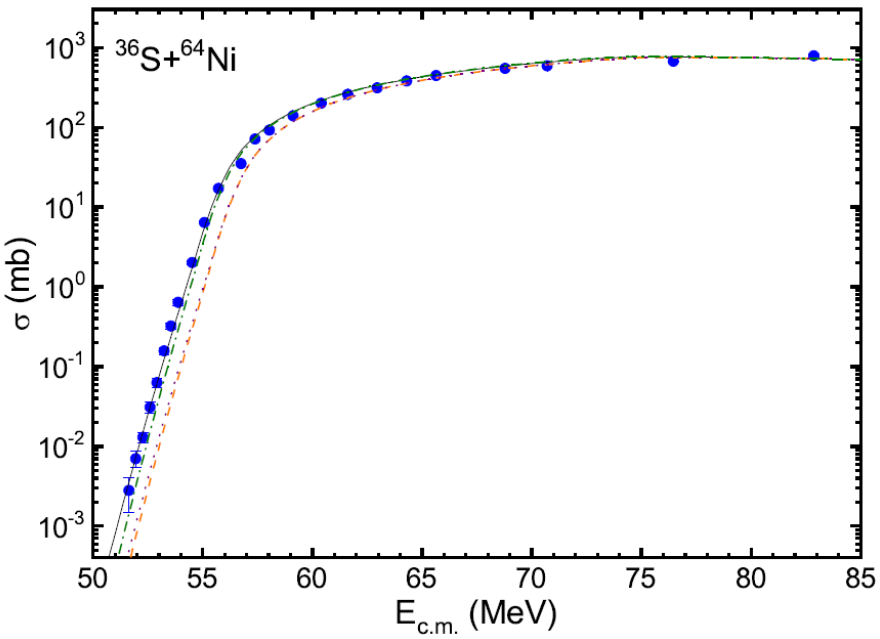

The experimental data are taken from [PRC 82, 064609 (2010)] (symbols). The cross sections calculated with the self-consistent nucleus-nucleus potential obtained with F_{ex} = - 4.484 are shown by dash-dotted line.

Modification of Skyrme EDF

$$\langle \Psi | H | \Psi \rangle = \int \mathcal{H}(\boldsymbol{r})\, d^3r\,,$$

with:

$$\mathcal{H} = \mathcal{K} + \mathcal{H}_0 + \mathcal{H}_3 + \mathcal{H}_{\rm eff} + \mathcal{H}_{\rm fin} + \mathcal{H}_{\rm so} + \mathcal{H}_{\rm sg} + \mathcal{H}_{\rm Coul}\,,$$

where $\mathcal{K} = \frac{\hbar^2}{2m}\tau$ is the kinetic-energy term, $\mathcal{H}_0$ a zero-range term, $\mathcal{H}_3$ the density-dependent term, $\mathcal{H}_{\rm eff}$ an effective-mass term, $\mathcal{H}_{\rm fin}$ a finite-range term, $\mathcal{H}_{\rm so}$ a spin–orbit term and $\mathcal{H}_{\rm sg}$ a term due to the tensor coupling with spin and gradient.

$$\mathcal{H}_0 = \frac{1}{4}t_0\left[(2+x_0)\,\rho^2 - (2x_0+1)\left(\rho_{\rm p}^2+\rho_{\rm n}^2\right)\right],$$

$$\mathcal{H}_3 = \frac{1}{24}t_3\rho^\sigma\left[(2+x_3)\,\rho^2 - (2x_3+1)\left(\rho_{\rm p}^2+\rho_{\rm n}^2\right)\right],$$

$$\mathcal{H}_{\rm eff} = \frac{1}{8}\left[t_1(2+x_1)+t_2(2+x_2)\right]\tau\rho + \frac{1}{8}\left[t_2(2x_2+1)-t_1(2x_1+1)\right]\left(\tau_{\rm p}\rho_{\rm p}+\tau_{\rm n}\rho_{\rm n}\right),$$

$$\mathcal{H}_{\rm fin} = \frac{1}{32}\left[3t_1(2+x_1)-t_2(2+x_2)\right](\nabla\rho)^2 - \frac{1}{32}\left[3t_1(2x_1+1)+t_2(2x_2+1)\right]\left[(\nabla\rho_{\rm p})^2+(\nabla\rho_{\rm n})^2\right],$$

$$\mathcal{H}_{\rm so} = \frac{1}{2}W_0\left[\boldsymbol{J}\cdot\nabla\rho + \boldsymbol{J}_{\rm p}\cdot\nabla\rho_{\rm p} + \boldsymbol{J}_{\rm n}\cdot\nabla\rho_{\rm n}\right],$$

$$\mathcal{H}_{\rm sg} = -\frac{1}{16}(t_1x_1+t_2x_2)\,\boldsymbol{J}^2 + \frac{1}{16}(t_1-t_2)\left[\boldsymbol{J}_{\rm p}^2+\boldsymbol{J}_{\rm n}^2\right].$$

Total densities are defined as $\rho = \rho_{\rm p}+\rho_{\rm n}$, $\tau = \tau_{\rm p}+\tau_{\rm n}$, $J = J_{\rm n}+J_{\rm p}$.

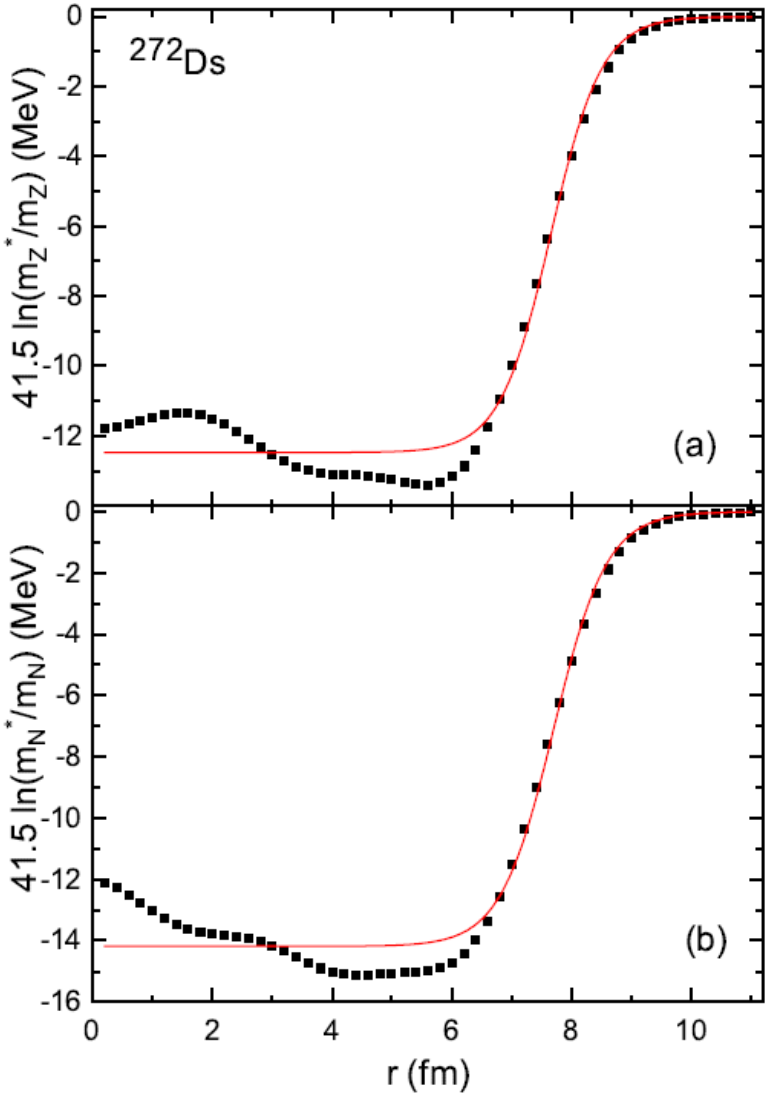

$$U_q^{(ls)}(r) = \frac{m_q^*(r)}{m_q} V_q^{(ls)}(r) = -\frac{1}{m_q}\frac{1}{r}\frac{\mathrm{d}\ln(m_q^*(r)/m_q)}{\mathrm{d}r}\mathbf{l}\cdot\mathbf{s}$$

$$U_q^{(ls)}(r) = -\kappa_q \frac{1}{r}\frac{\mathrm{d}}{\mathrm{d}r}\frac{V_q^0}{1+\exp[(r-R'_q)/a'_q]}\mathbf{l}\cdot\mathbf{s},$$

where the constants $\kappa_N = 0.27$ fm^2 and $\kappa_Z = 0.19$ fm^2, $a'_N = 0.46$ fm and $a'_Z = 0.435$ fm, and the radii R'_q are calculated with $r'_{0N} = 1.19$ fm and $r'_{0Z} = 1.18$ fm.

The spin-orbit strength ~ κ_q / a'_q is about 15% larger than that in EPJA 57, 89 (2021). The sum and difference of scalar and vector potentials result in the differences of r_{0q} and a_q from r'_{0q} and a'_q, respectively.

Spin-orbit strength is related to effective mass and

$$W_0 = \frac{1}{6}(3t_1 + (5 + 4x_2)t_2)$$

$$\mathcal{E}_{int}(\rho_0,\rho_1) = \frac{1}{2}\left(\rho_0^2 V_0(\rho_0) + \rho_1^2 V_1(\rho_0)\right)$$

including an isoscalar (V_0) and an isovector (V_1) interaction vertex. Variation leads to the isoscalar and isovector potentials

$$\begin{aligned} U_s(\rho_0,\rho_1) &= \frac{\delta \mathcal{E}_{int}}{\delta \rho_0} \\ &= \rho_0 V_0(\rho_0) + \frac{1}{2}\rho_0^2 \frac{\partial V_0(\rho)}{\partial \rho}\bigg|_{\rho_0} + \frac{1}{2}\rho_1^2 \frac{\partial V_1(\rho)}{\partial \rho}\bigg|_{\rho_0} \end{aligned} \tag{35}$$

$$U_v(\rho_0,\rho_1) = \frac{\delta \mathcal{E}_{int}}{\delta \rho_1} = \rho_1 V_1(\rho). \tag{36}$$

The proton and neutron potentials are recovered by

$$U_{p,n}(\rho_0,\rho_1) = U_s(\rho_0,\rho_1) \mp U_v(\rho_0,\rho_1). \tag{37}$$

Suppose that $U_{p,n}$ and therefore by Eq. (37) also $U_{s,v}$ are known from other sources, e.g. from a fit to nuclear ground-state properties and that the corresponding single-particle Schrödinger equations have been solved such that the densities are available. Then, by inversion we can reconstruct the EDF by means of the self-consistency relations

It is worthwhile to point at a few advantages of this inversion method: First, we do not constrain the interactions by a pre-chosen functional ansatz which may be biased by certain model assumptions. Second, the inversion approach provides the theoretically well defined scheme for the extraction of the proper EDF which corresponds to the phenomenological potentials. This is achieved by removing the rearrangement self-energies which are inescapably contained in the phenomenological potentials.

Summary

- If the neutron shell closure appears at a level with large orbital momentum, the nuclear diffuseness decreases.

- The non-covariant SC approach provides a good description of fusion reactions with light nuclei. Without adjusting parameters, there is a good description of sub-barrier fusion.

- EDF for the SC calculation of the Coulomb barriers